Acta Mechanica Slovaca **29 (4): 36 - 43,** December **2025**
https://doi.org/10.21496/ams.2026.005

Acta Mechanica Slovaca
ISSN 1335-2393
www.actamechanica.sk

Vibration-Controlled Jet Breakup for Monodisperse Droplet Formation in a Rotating Granulation System

Dmitry Zabitsky[1], Ruslan Ostroha[1,*]

[1] Sumy State University, 116, Kharkivska St., 40007, Sumy, Ukraine

Abstract: This study examines vibration-controlled jet breakup and its role in droplet formation in a rotating granulation system. A 2^2 full factorial experimental design was used to evaluate the combined influence of actuator position (5÷30 mm) and liquid column height (120÷450 mm) on the forced vibration regime. A regression model confirmed the presence of structural-dynamic interaction between these parameters. Experimental observations showed that stable monodisperse droplets were obtained at a liquid column height of 380 mm, vibration frequency of 380 Hz, and amplitude of 100 μm, where periodic pinch-off occurred without satellite droplets. Reducing the liquid height to 280 mm and lowering the excitation frequency to 220 Hz led to satellite droplet formation, while a regime of 800 Hz and 50 μm amplitude resulted in polydisperse breakup. The results show that monodispersity is achieved only within a limited combination of structural configuration and vibration parameters, providing a basis for optimizing vibration-assisted granulation processes.

Keywords: oscillatory forcing, droplet formation dynamics, size distribution control, vibration tuning, granule uniformity, hydrodynamic response, parametric interaction, process optimization.

1.Introduction

The disintegration of liquid and molten jets plays a key role in many industrial technologies, including spray formation, melt granulation, and droplet-based material processing. The manner in which a jet breaks up determines droplet size distribution and the degree of monodispersity, which in turn influence the stability of the technological regime and the properties of the final product [1, 2].

Mechanically, jet breakup results from the interaction between inertial, viscous, and capillary forces. According to the classical Rayleigh-Plateau theory, small surface disturbances along the jet grow under the action of surface tension and eventually lead to droplet formation. In real industrial systems, however, the jet is rarely free from external influence. Mechanical excitation, especially in vibration-assisted devices, modifies the natural instability development and can either enhance or suppress certain perturbation modes [3, 4].

In vibration-based granulation units, oscillations generated by an actuator are transmitted through the liquid column before reaching the jet formation zone. Under such conditions, not only the excitation frequency but also the geometrical configuration of the system becomes important. The vertical position of the actuator and the height of the liquid column affect the way mechanical energy is transferred to the flowing medium and may alter the resulting vibration regime.

Although jet instability has been widely studied, the combined influence of structural parameters and forced excitation conditions in practical granulation systems

*** Corresponding author:** Ruslan Ostroha, ***E-mail address:*** *r.ostroga@pohnp.sumdu.edu.ua*

has not been sufficiently clarified. In particular, the possible interaction between actuator position and liquid column height, and its effect on the resulting forced vibration frequency, requires systematic experimental analysis.

2. Problem Statement

The formation of droplets from liquid jets belongs to the classical problems of hydrodynamics that have attracted scientific attention for more than a century. The theoretical foundations of jet breakup were established through the experimental observations of Plateau and the analytical treatment by Rayleigh, who demonstrated that long-wave axisymmetric disturbances inevitably lead to the disintegration of a cylindrical jet under the action of surface tension [5, 6]. This Rayleigh-Plateau instability model remains a fundamental reference in the analysis of liquid jet breakup.

Further refinement of the theory was introduced by Tomotika, who incorporated viscous effects into the stability analysis and showed that viscosity significantly influences disturbance growth rates and breakup times [7]. These findings are particularly relevant for industrial melts, including fertilizer melts and polymer systems, whose rheological properties differ from ideal inviscid fluids.

The breakup process is commonly described using dimensionless parameters such as the Weber number, Reynolds number, Ohnesorge number, and capillary number, which characterize the relative contributions of inertial, viscous, and surface tension forces [8]. These criteria provide a theoretical framework for understanding instability development in free jets.

In industrial production of mineral fertilizers from melts, the prilling method remains one of the most reliable and economically efficient technologies [9, 10]. In tower-type granulation systems, melt streams are introduced at the top of the tower and disintegrate into droplets during free fall (Fig. 1). Under such conditions, the jet breakup mechanism directly determines granule size distribution, uniformity, and process stability [11].

Depending on the technological configuration, both tower and centrifugal granulators are used in practice [12]. In vibration-assisted systems, external mechanical excitation is applied to improve droplet uniformity and stabilize the granulation regime [13]. Experimental observations indicate that vibration may significantly influence droplet size distribution compared to non-vibrational operation.

However, the disintegration of melt jets under mechanical excitation remains a complex and multi-factor process [14, 15]. Along with intrinsic hydrodynamic instability, externally imposed oscillations modify the dynamic response of the system. The effectiveness of such excitation depends not only on nominal frequency and amplitude, but also on structural configuration and geometric parameters of the granulator [16].

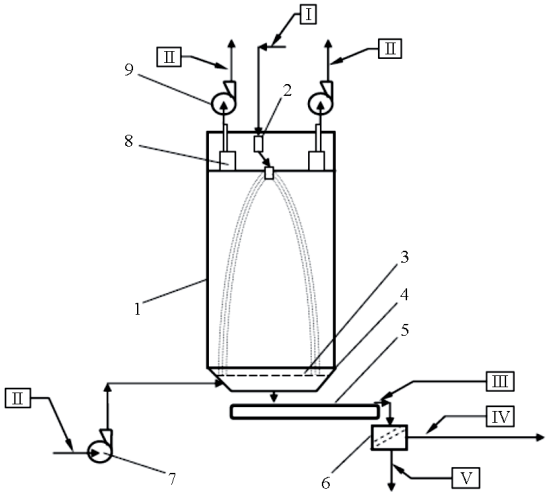

Figure 1: Schematic diagram of mineral fertilizer production by the prilling method: 1 – granulation tower; 2 – melt supply system to the granulator; 3 – fluidized-bed granule cooler; 4 – collecting cones; 5 – conveyor; 6 – size classifier (screen); 7 – pressure fan; 8 – air cleaning unit; 9 – exhaust fans; I – fertilizer melt; II – air; III – granule discharge from the tower; IV – commercial granules; V – off-spec granules for reprocessing

Although numerous studies have investigated natural jet breakup and externally forced perturbations [17–19], the combined influence of structural parameters and forced vibration conditions in practical vibration-assisted granulators has not been systematically quantified. In particular, the interaction between actuator position and liquid column height, and its effect on the resulting forced vibration regime, remains insufficiently investigated.

Therefore, the problem addressed in this study is to determine the quantitative influence of structural parameters on the forced vibration regime in a vibration-assisted granulation system and to evaluate their interaction effect using a structured experimental design approach.

3. Research Methodology

To quantify the influence of structural parameters on the forced vibration regime formulated in Section 2, a full factorial experimental design of type 2^2 was implemented.

In a full factorial design (FFD), all possible combinations of factor levels are tested, allowing simultaneous evaluation of main effects and interaction effects between variables. For a design with k factors studied at n levels, the total number of experimental runs N is given by:

$$N = n^k, \tag{1}$$

where n – the number of levels for each factor; k – the number of factors under investigation ($j=1,2,...,k$).

In a 2^2 full factorial design, each of the $k = 2$ factors are studied at $n = 2$ levels, typically denoted as low (-1) and high $(+1)$ values, representing the range of parameter variation. This approach enables the identification of not only the main effects of each factor but also their possible interaction effects, which is essential for optimizing the technological parameters of the process.

The selected factors for this experiment were vibration transmission method and vibration frequency applied to the working body of the dispersing system. These parameters were hypothesized to significantly affect granule uniformity, mechanical strength, and the stability of the granulation regime.

In this study, we investigated the influence of actuator vibration frequency on the quality parameters of the granulation process, using a granulator equipped with a circular actuator of 100 mm in diameter and 1 mm in thickness. Two primary factors were selected for the factorial analysis:

– z_1 – *the vertical distance from the bottom of the vessel to the actuator plate, varied within the range of 5 mm to 30 mm;*

– z_2 – *the height of the water column in the working basket, varied between 120 mm and 450 mm.*

To examine the effects of these parameters, we applied a 2^2 full factorial experimental design, which requires four individual experiments ($N = 2^2 = 4$) corresponding to all possible combinations of factor levels.

Before constructing the experimental matrix, factor values were coded to normalize their ranges. The coding was performed using the standard transformation equations:

$$x_1 = \frac{z_1 - z_1^0}{\Delta z_1}, \tag{2}$$

$$x_2 = \frac{z_2 - z_2^0}{\Delta z_2}, \tag{3}$$

where

$$z_1^0 = \frac{z_1^{\max} + z_1^{\min}}{2} = \frac{30+5}{2} = 17.5 \ \ mm, \tag{4}$$

$$\Delta z_1 = \frac{z_1^{\max} - z_1^{\min}}{2} = \frac{30-5}{2} = 12.5 \ \ mm, \tag{5}$$

$$z_2^0 = \frac{z_2^{\max} + z_2^{\min}}{2} = \frac{450+120}{2} = 285 \ \ mm, \tag{6}$$

$$\Delta z_2 = \frac{z_2^{\max} - z_2^{\min}}{2} = \frac{450-120}{2} = 165 \ \ mm, \tag{7}$$

$z_j^{\max}, z_j^{\min}, j = 1,2$ – upper and lower bounds of the corresponding factor.

The transformation enables the use of normalized dimensionless variables x_1 and x_2 $(-1$ and $+1)$, which are essential for analysing the effects and interactions within the factorial design framework. These values represent the design space boundaries and provide the foundation for further evaluation of how vibration parameters affect the monodispersity and structural integrity of the granules.

The point $\left(z_1^0; z_2^0\right)$ represents the centre of the design space, also referred to as the base (or reference) level of the experimental plan. The quantities $\Delta z_1, \Delta z_2$ denote the variation intervals along the axes z_1 and z_2, respectively.

As follows from equations (2–7), for the coded variables x_1 and x_2, the lower level corresponds to -1, the upper level to $+1$, while the centre point of the design corresponds to 0.

The design matrix of the 2^2 full factorial experiment is presented in Table 1 and can be visualized in a dimensionless coordinate system as the four vertices of a square (Fig. 2). Each vertex represents a unique combination of factor levels, enabling both the identification of main effects and the analysis of interaction between the two studied variables.

To further analyse the experimental results, we computed the coefficients of a first-order linear regression model with interaction terms. The regression equation is represented as:

$$\hat{y} = b_0 + b_1 \cdot x_1 + b_2 \cdot x_2. \tag{8}$$

Table 1: Full Factorial Design of Type 2^2

Experiment No.	Factors in natural scale		Factors in dimensionless scale		Actuator working frequency, Hz
	z_1 or Δ, mm	z_2 or H, mm	x_1	x_2	
1	5	120	−1	−1	$y_1 = 318 \pm 0.5$
2	5	450	−1	+1	$y_2 = 250 \pm 0.5$
3	30	120	+1	−1	$y_3 = 360 \pm 0.5$
4	30	450	+1	+1	$y_4 = 434 \pm 0.5$

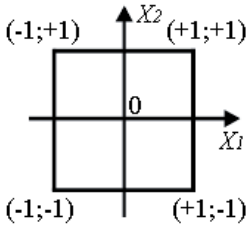

Figure 2: Full factorial design 2^2 represented in the normalized coordinate system

In order to calculate the intercept b0, the experimental plan matrix must include a column for the fictitious variable $x_0=1$, representing the constant term. According to the principles of mathematical statistics, when using a full factorial design, the regression coefficients can be determined using the method of least squares.

Each coefficient b_i is computed as the scalar product of the column vector of the response values y and the corresponding column of the design matrix (for x_i in coded values), divided by the total number of experiments. This approach allows accurate estimation of main and interaction effects within the design.

The extended planning matrix of the 2^2 full factorial design, including interaction terms, is presented in Table 2.

Table 2: Extended Design Matrix for the 2^2 Full Factorial Experiment

Experiment No.	x_0	x_1	x_2	$x_1 \cdot x_2$	y, Hz
1	+1	−1	−1	+1	$y_1 = 318 \pm 0.5$
2	+1	−1	+1	−1	$y_2 = 250 \pm 0.5$
3	+1	+1	−1	−1	$y_3 = 360 \pm 0.5$
4	+1	+1	+1	+1	$y_4 = 434 \pm 0.5$

$$x_2.b_j = \frac{\sum_{i=1}^{N} x_{ji} \cdot y_i}{N}, \tag{9}$$

$$b_0 = \frac{\sum_{i=1}^{N} x_{0i} \cdot y_i}{N} = \frac{\left(x_0\right)_1 \cdot y_1 + \left(x_0\right)_2 \cdot y_2 + \left(x_0\right)_3 \cdot y_3 + \left(x_0\right)_4 \cdot y_4}{4} = \frac{y_1 + y_2 + y_3 + y_4}{4} = \frac{318 + 250 + 360 + 434}{4} = 340.5 \text{ Hz}, \tag{10}$$

$$b_1 = \frac{\sum_{i=1}^{N} x_{1i} \cdot y_i}{N} = \frac{\left(x_1\right)_1 \cdot y_1 + \left(x_1\right)_2 \cdot y_2 + \left(x_1\right)_3 \cdot y_3 + \left(x_1\right)_4 \cdot y_4}{4} = \frac{-y_1 - y_2 + y_3 + y_4}{4} = \frac{-318 - 250 + 360 + 434}{4} = 56.5 \text{ Hz}, \tag{11}$$

$$b_2 = \frac{\sum_{i=1}^{N} x_{2i} \cdot y_i}{N} = \frac{\left(x_2\right)_1 \cdot y_1 + \left(x_2\right)_2 \cdot y_2 + \left(x_2\right)_3 \cdot y_3 + \left(x_2\right)_4 \cdot y_4}{4} = \frac{-y_1 + y_2 - y_3 + y_4}{4} = \frac{-318 + 250 - 360 + 434}{4} = 1.5 \text{ Hz}, \tag{12}$$

$$b_{12} = \frac{\sum_{i=1}^{N} \left(x_1 \cdot x_2\right)_i \cdot y_i}{N} = \frac{1}{4}\left[\left(x_1 \cdot x_2\right)_1 \cdot y_1 + \left(x_1 \cdot x_2\right)_2 \cdot y_2 + \left(x_1 \cdot x_2\right)_3 \cdot y_3 + \left(x_1 \cdot x_2\right)_4 \cdot y_4\right] = \frac{y_1 - y_2 - y_3 + y_4}{4} = \frac{318 - 250 - 360 + 434}{4} = 35.5 \text{ Hz}. \tag{13}$$

Based on the experimental data and the calculated coefficients, the linear regression model describing the actuator vibration frequency $(\hat{y})$ in the granulator as a function of the coded factors x_1, x_2, and their interaction is given by:

$$
\begin{aligned}
&\hat{y} = b_0 + b_1 \cdot x_1 + b_2 \cdot x_2 + b_{12} \cdot x_1 \cdot x_2 = \\
&= 340.5 + 56.5 \cdot x_1 + 1.5 \cdot x_2 + 35.5 \cdot x_1 \cdot x_2 = \\
&= b_0 + b_1 \cdot \frac{z_1 - z_1^0}{\Delta z_1} + b_2 \cdot \frac{z_2 - z_2^0}{\Delta z_2} + b_{12} \cdot \frac{z_1 - z_1^0}{\Delta z_1} \cdot \frac{z_2 - z_2^0}{\Delta z_2} = \\
&= 340.5 + 56.5 \cdot \frac{z_1 - 17.5}{12.5} + 1.5 \cdot \frac{z_2 - 285}{165} + 35.5 \cdot \frac{z_1 - 17.5}{12.5} \cdot \frac{z_2 - 285}{165} = \\
&= 340.5 + 56.5 \cdot \frac{\Delta - 17.5}{12.5} + 1.5 \cdot \frac{H - 285}{165} + 35.5 \cdot \frac{\Delta - 17.5}{12.5} \cdot \frac{H - 285}{165} = \\
&= 340.5 + 4.52 \cdot \left(\Delta - 17.5\right) + 0.0(09) \cdot \left(H - 285\right) + 2.84 \cdot (\Delta - 17.5) \times \\
&\times \left(H - 285\right) = 14423.31 - 804.88 \cdot \Delta - 49.69 \cdot H + 2.84 \cdot \Delta \cdot H.
\end{aligned}
\tag{14}
$$

This expression enables preliminary prediction of the forced vibration frequency of the actuator (in Hz) for preset values of the distance between the bottom and the actuator plate, as well as the height of the water column in the basket, under the assumption of a stable and continuous granulation process.

Such a model provides a practical tool for pre-configuring operating conditions in industrial or pilot-scale systems, allowing for the fine-tuning of key parameters to achieve optimal granule formation without disrupting hydrodynamic equilibrium.

The vibration condition of the granulation equipment was assessed using a certified portable vibration analysis system designed for industrial diagnostics and condition monitoring. The system complied with metrological standards and was calibrated in accordance with national regulations, as confirmed by a valid verification certificate issued by an accredited calibration laboratory.

Standard piezoelectric accelerometers of PA023 type were used for data acquisition. These sensors were mounted at key structural points of the granulator to capture vibration signals along the principal axes of dynamic excitation.

Subsequent data processing and analysis were performed using specialized vibration analysis software, which supported real-time signal monitoring and post-processing. The identification of characteristic frequencies and amplitude peaks was carried out using an integrated frequency calculator tool, allowing for the detection of potential resonance conditions and deviations from nominal operational behaviour.

The operational vibration state of the equipment was monitored by vertically mounting the accelerometer on a threaded probe at the central, hermetically sealed point on the bottom of the granulator basket. This setup, compliant with ISO 5348:2021, ensured accurate detection of dominant axial vibrations transmitted through the actuator and working medium. The chosen mounting method provided stable sensor contact, minimal signal distortion, and high repeatability of measurements under identical experimental conditions.

The vibration assessment was conducted in accordance with applicable standards over the 2 Hz to 1 kHz frequency range, with the primary monitored parameter being overall vibration velocity (mm/s, RMS). To further analyse dynamic behaviour and detect potential resonances or mechanical irregularities, spectral measurements of both vibration velocity and acceleration (m/s^2, RMS) were performed at all key points. This dual-parameter approach provided a comprehensive frequency-domain evaluation, capturing both low-frequency structural responses and high-frequency disturbances, thus offering a detailed overview of the granulation unit's vibrational performance.

4. Results

The regression model obtained from the 2^2 full factorial design provides a quantitative description of the actuator forced vibration frequency as a function of the structural parameters z_1 and z_2. The inclusion of the interaction term reveals that the effect of each factor cannot be considered independently, as the resulting vibration regime depends on their combined configuration.

Analysis of the regression coefficients indicates that both the actuator position and the liquid column height exert a significant influence on the measured vibration frequency. However, the magnitude and

direction of this influence vary depending on the specific combination of factor levels, confirming the presence of structural-dynamic coupling within the system.

The interaction effect demonstrates that certain geometric configurations promote more efficient transmission of oscillatory energy through the liquid column, leading to stable and repeatable vibration regimes. These configurations correspond to operating conditions under which monodisperse droplet formation was experimentally observed.

Experimental visualization of the jet breakup process under selected operating conditions (liquid column height 380 mm, vibration frequency 380 Hz, amplitude 100 µm) confirmed the formation of a stable monodisperse disintegration regime (Fig. 3). The liquid jet exhibited periodic surface perturbations characterized by alternating radial expansion and contraction zones. As the oscillatory regime stabilized, the contraction zones diminished, resulting in uniform primary droplet formation without satellite droplets.

At a liquid column height of 280 mm, with a forced vibration frequency of 220 Hz and an amplitude of 100 µm, the jet exhibited a different breakup regime compared to the monodisperse case described above (Fig. 4). The disintegration process was accompanied by the formation of primary droplets together with satellite droplets.

At a reduced liquid column height of 280 mm, combined with a vibration frequency of 800 Hz and an amplitude of 50 µm, the jet exhibited a different disintegration pattern (Fig. 5). The breakup process resulted in a polydisperse droplet distribution with the formation of satellite droplets.

To provide a structured comparison of the investigated operating conditions and the corresponding jet breakup regimes, the main experimental configurations are summarized in Table 3. The table presents the selected structural parameters and vibration characteristics together with the experimentally observed disintegration patterns.

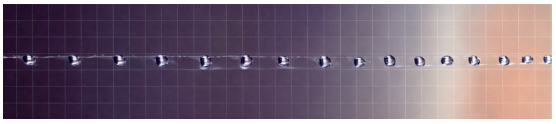

Figure 3: Experimental visualization of jet breakup at a vibration frequency of 380 Hz and amplitude of 100 µm, with a liquid column height of 380 mm (grid spacing – 4 mm)

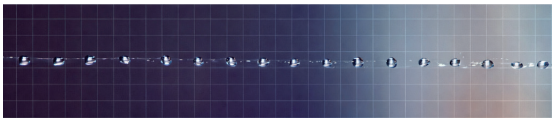

Figure 4: Experimental visualization of jet breakup at a vibration frequency of 220 Hz and amplitude of 100 µm, with a liquid column height of 280 mm (grid spacing – 4 mm)

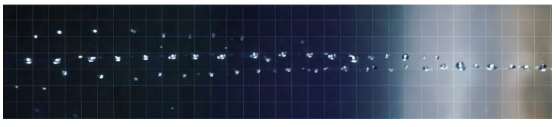

Figure 5: Experimental visualization of jet breakup at a vibration frequency of 800 Hz and amplitude of 50 µm, with a liquid column height of 280 mm (grid spacing – 4 mm)

5. Discussion

The experimental results demonstrate that the formation of a narrow granulometric distribution in a vibration-assisted granulator is governed by the coupled influence of structural and dynamic parameters. In particular, the liquid column height and the actuator position determine the effective transmission of vibrational energy to the jet formation zone, which directly affects the stability of droplet detachment.

The stable monodisperse regime observed at a liquid column height of 380 mm and a vibration frequency of 380 Hz indicates the existence of a structural-dynamic resonance-like condition within the system. Under these parameters, the oscillatory excitation appears to synchronize with the natural hydrodynamic response of the liquid jet. This

Table 3: Summary of Investigated Vibration Regimes and Observed Jet Breakup Patterns

Regime	Liquid column height, mm	Vibration frequency, Hz	Amplitude, µm	Observed breakup pattern
1	380	380	100	Stable monodisperse droplets
2	280	220	100	Primary droplets with satellite droplets
3	280	800	50	Polydisperse droplet distribution with satellite formation

synchronization promotes periodic and coherent pinch-off, resulting in uniform primary droplets and suppression of secondary satellite formation.

In contrast, reducing the liquid column height to 280 mm significantly alters the dynamic response of the system. At a lower excitation frequency (220 Hz), the vibrational energy transmitted through the liquid column is insufficient to fully stabilize the jet surface disturbances. As a result, the droplet detachment process becomes partially desynchronized, leading to the appearance of satellite droplets and increased dispersion in droplet size.

A further deviation from optimal conditions was observed at high excitation frequency (800 Hz) combined with low amplitude (50 μm). In this configuration, the imposed frequency exceeds the system's effective hydrodynamic response capacity. The insufficient vibration amplitude limits coherent energy transfer, leading to irregular surface perturbations and a polydisperse breakup regime. This behaviour suggests that frequency alone does not determine stability; rather, a balanced combination of frequency, amplitude, and liquid column height is required.

These findings confirm that the narrow granulometric composition of granules in a rotating vibration granulator cannot be ensured solely by increasing excitation intensity. Instead, monodisperse droplet formation occurs within a limited operational window defined by the interaction of geometric configuration and vibrational forcing. Outside this window, either under-excitation or mismatched excitation parameters result in destabilized jet breakup and broader particle size distribution.

From a mechanical standpoint, the structural parameters of the granulator define the boundary conditions for wave propagation within the liquid column. The height of the working fluid layer influences the development and amplification of surface perturbations, while the actuator position controls the initial excitation pattern. Their combined effect determines whether oscillations reinforce periodic pinch-off or amplify uncontrolled instabilities.

6. Conclusions

1. The application of a 22 full factorial experimental design enabled a quantitative assessment of the influence of actuator position and liquid column height on the forced vibration regime. The obtained regression model confirmed the presence of structural-dynamic coupling, demonstrating that the vibration frequency is determined not by isolated parameters, but by their combined configuration.

2. It has been experimentally established that stable monodisperse droplet formation occurs only within a limited range of vibration parameters, where the excitation frequency, amplitude, and liquid column height are mutually coordinated. Under these conditions, the jet disintegrates without satellite droplets, ensuring a narrow granulometric distribution.

3. A decrease in liquid column height or deviation from the optimal excitation frequency leads to the appearance of satellite droplets and transition to a less stable regime. At excessively high frequencies combined with insufficient amplitude, a polydisperse droplet distribution is formed, indicating the loss of synchronization between forced excitation and natural jet instability.

4. The results confirm that the monodispersity of granules in a vibration-assisted rotating granulator is governed by the interaction between structural parameters of the system and the imposed vibrational regime. This interaction defines a stability window within which energy transfer to the jet core is most efficient and droplet detachment becomes dynamically synchronized.

5. The developed regression model and experimental observations provide a practical foundation for the formulation of engineering recommendations aimed at improving granule size uniformity, process stability, and energy efficiency in industrial granulation systems.

Acknowledgments

This project has received funding from the European Union's Horizon 2020 research and innovation programme under grant agreement No. 871072. This work was carried out within the framework of the project "Development of Technological Foundations for Obtaining Complex Mixed Fertilizers with Monodisperse Composition" (State Reg. No. 0125U000500), funded by the Ministry of Education and Science of Ukraine.

References

1. Marmottant, P. & Villermaux, E. (2004). On spray formation. Journal of Fluid Mechanics, 498, 73–111. https://doi.org/10.1017/S0022112003006529
2. Eggers, J. & Villermaux, E. (2008). Physics of liquid jets. Reports on Progress in Physics, 71, 036601. https://doi.org/10.1088/0034-4885/71/3/036601
3. Luo, L., Liu, Y., Li, X. & Wang, Z. (2025). Review on the recent numerical studies of liquid atomization. Applied Sciences, 15, 4928. https://doi.org/10.3390/app15094928
4. Kirar, P.K., Kumar, N. & Sahu, K.C. (2024). Dynamics of jet breakup and the resultant drop size distribution: effect of nozzle size and impingement velocity. Physics of Fluids, 36(10), 102108. https://doi.org/10.1063/5.0225452
5. Plateau, J.A.F. (1873). Statique expérimentale et théorique

des liquides soumis aux seules forces moléculaires. Gauthier-Villars, Paris, France.
6. Rayleigh, L. (1878). On the instability of jets. Proceedings of the London Mathematical Society, 1(10), 4–13. https://doi.org/10.1112/plms/s1-10.1.4
7. Tomotika, S. (1935). On the instability of a cylindrical thread of a viscous liquid surrounded by another viscous fluid. Proceedings of the Royal Society of London, Series A, 150, 322–337. https://doi.org/10.1098/rspa.1935.0104
8. Grant, R.P. & Middleman, S. (1966). Newtonian jet stability. AIChE Journal, 12(4), 669–678. https://doi.org/10.1002/aic.690120404
9. Gezerman, A.O. (2020). Mathematical modeling for prilling processes in ammonium nitrate production. Engineering Reports, 2, e12173. https://doi.org/10.1002/eng2.12173
10. Nichvolodin, K. & Sklabinskyi, V. (2023). Determination of the heat transfer coefficient between pellets and air during the modernization of a pelletizing tower based on industrial research. Technology Audit and Production Reserves, 6, 18–21. https://doi.org/10.15587/2706-5448.2023.293264
11. Skydanenko, M., Sklabinskyi, V., Nadhem, A.-K.M. & Nichvolodin, K. (2021). Determination of granule (prill) movement modes in the prilling tower for mineral fertilizer production. Technology Audit and Production Reserves, 5(3(61)), 6–9. https://doi.org/10.15587/2706-5448.2021.241142
12. Muhammad, A., Rahmanian, N. & Pendyala, R. (2013). Flow analysis of melted urea in a perforated rotating bucket. Applied Mechanics and Materials, 372, 340–345. https://doi.org/10.4028/www.scientific.net/AMM.372.340
13. Ha, K.T.V., Nguyen, T.-A., Nguyen, Q.-L., Dang, V.-V., Dang, V.-H., Van, H.-L. & Pham, L.-N.T. (2023). Two-phase Stefan problem for the modeling of urea prilling tower. Engineering Proceedings, 37, 122. https://doi.org/10.3390/ECP2023-14745
14. Zhang, T., Song, X., Kai, X., He, Y. & Li, R. (2023). Numerical simulation on primary breakup characteristics of liquid jet in oscillating crossflow. Aerospace, 10(12), 991. https://doi.org/10.3390/aerospace10120991
15. Song, Y., Zhou, T., Bai, R., Zhang, M. & Yang, H. (2023). Review of CFD-DEM modeling of wet fluidized bed granulation and coating processes. Processes, 11, 382. https://doi.org/10.3390/pr11020382
16. Eggers, J. (2005). Drop formation – an overview. Zeitschrift für Angewandte Mathematik und Mechanik, 85(6), 400–410. https://doi.org/10.1002/zamm.200410193
17. Yang, L.Y., Zheng, Q. & Yu, A. (2022). A continuum model for the segregation of bidisperse particles in a blade mixer. AIChE Journal, 68(8), e17734. https://doi.org/10.1002/aic.17734
18. Liu, Z., Li, Z., Liu, J., Wu, J., Yu, Y. & Ding, J. (2022). Numerical study on primary breakup of disturbed liquid jet sprays using a VOF model and LES method. Processes, 10(6), 1148. https://doi.org/10.3390/pr10061148
19. Kant, K. & Banerjee, R. (2022). Effect of non-Newtonian rheology on bag breakup at different liquid to gas density ratios. In Proceedings of the 7th Thermal and Fluids Engineering Conference (TFEC), 15–18 May 2022, Las Vegas, NV, USA. https://doi.org/10.1615/TFEC2022.nma.040888